# Influence of $J_c(B, T)$ Characteristics on the Pulsed Field Magnetization of REBaCuO Disk Bulks

Tatsuya Hirano, Keita Takahashi, Fumiya Shimoyashiki, Hiroyuki Fujishiro, Tomoyuki Naito, and Mark D. Ainslie, *Senior Member, IEEE*

***Abstract*—The trapped field properties during pulsed-field magnetization (PFM) have been investigated numerically using three different assumptions relating to the $J_c(B, T)$ characteristics (Jirsa, Kim, and Bean models) and compared with experimental results. The trapped field properties using the Jirsa model with the so-called "peak effect," in which a realistic $J_c(B, T)$ is assumed, rather than the Kim model, result in a more realistic numerical simulation. The trapped field properties using a Kim model with a monotonically decreasing $J_c(B)$ also show similar results to those using the Jirsa model. The trapped field properties using a Bean model, for which $J_c$ is independent of magnetic field, are not necessarily enhanced because of a larger temperature rise. The numerical results suggest it is necessary to fabricate REBaCuO bulks with $J_c(B, T)$ characteristics with moderate magnetic field and temperature dependences to enhance the trapped field by PFM.**

***Index Terms*—$J_c(B, T)$ characteristics (Jirsa model, Kim model, Bean model), numerical simulation, pulsed-field magnetization (PFM), REBaCuO bulk.**

## I. Introduction

REBaCuO (RE: rare earth element or Y) superconducting bulks have a significant potential as strong trapped field magnets (TFMs), which can be used in a variety of engineering applications. Pulsed-field magnetization (PFM) is a practical magnetizing technique to realize TFMs without the need for a superconducting magnet, in contrast to field-cooled magnetization (FCM), because of its relatively compact, inexpensive, and mobile experimental setup. However, the trapped field by PFM is much lower than that by FCM because of a large temperature rise due to the rapid and dynamic motion of magnetic flux. Several improvements have been made experimentally and numerically for the PFM technique to enhance the trapped field; the insertion of soft iron yoke from a magnetic point of view [1], and the multipulse application from a thermal point of view [2], [3]. The trapped field of TFMs by PFM is determined by a complex relationship between $J_c(B, T)$, the thermal properties (specific heat and thermal conductivity) of the bulk material, cooling condition (the thermal contact and magnetizing temperature), the rise time of the magnetic pulse, etc. In general, the results from numerical simulation can provide insights that are difficult to realize experimentally, and can also verify experimental results. Therefore, it is a powerful tool to analyze such behaviors and predict the performance of bulk superconductors as TFMs. [4].

Several numerical analyses have been performed to understand the magnetizing mechanism and to enhance the trapped field by PFM [5]. There are several $J_c(B)$ characteristic models used in the literature. In the Jirsa model, experimental $J_c(B)$ characteristics that exhibit a peak effect are fitted at each temperature [6]. In the classical Bean model, the $J_c$ value is independent of magnetic field at each temperature [7]. In the Kim model, the $J_c(B)$ characteristics monotonically decrease with increasing magnetic field at each temperature [8]. Until now, numerical simulations during PFM using three different $J_c(B, T)$ characteristics have not been investigated using an identical numerical model. Furthermore, such simulations have not been compared with the experimental results.

In this paper, to understand the complex trapped field mechanism and to clarify the desirable $J_c(B, T)$ characteristics of the REBaCuO bulk, we performed numerical simulations of PFM for a REBaCuO disk bulk using three different assumptions of the $J_c(B, T)$ characteristics: the Jirsa model [6], the Bean model [7], and the Kim model [8]. These numerical results are compared with experimental results. The most desirable approach to enhance the trapped field, as well as the most appropriate assumptions for the simulation closely to reproduce the experimentally observed results are discussed from the viewpoints of the magnetic and thermal behavior during PFM.

## II. Experimental Setup and Numerical Simulation Framework

### A. Experimental Setup

A GdBaCuO disk bulk superconductor (Nippon Steel & Sumitomo Metal) of 64 mm in outer diameter (O.D.) and 20 mm in

Manuscript received January 14, 2018; revised August 25, 2018; accepted September 16, 2018. Date of publication October 1, 2018; date of current version January 8, 2019. This work was supported in part by JSPS KAKENHI under Grant 15K04646. The work of M. D. Ainslie was support by Engineering and Physical Sciences Research Council (EPSRC) Early Career Fellowship EP/P020313/1. This paper was recommended by Associate Editor M. Izumi. *(Corresponding author: Tatsuya Hirano.)*

T. Hirano, K. Takahashi, F. Shimoyashiki, H. Fujishiro, and T. Naito are with the Department of Physical Science and Materials Engineering, Faculty of Science and Engineering, Iwate University, Morioka 020-8551, Japan (e-mail: g0318132@iwate-u.ac.jp; fujishiro@iwate-u.ac.jp).

M. D. Ainslie is with the Bulk Superconductivity Group, Department of Engineering, University of Cambridge, Cambridge CB2 1PZ, U.K. (e-mail: mark.ainslie@eng.cam.ac.uk).

Color versions of one or more of the figures in this paper are available online at http://ieeexplore.ieee.org.

Digital Object Identifier 10.1109/TASC.2018.2872819

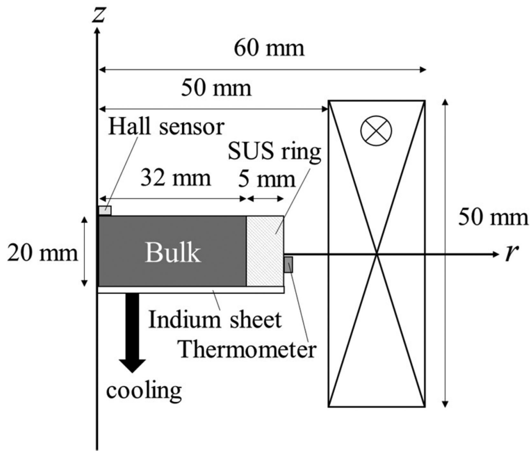


Fig. 1. Schematic view and the dimensions of the experimental setup for the PFM experiments using a magnetizing solenoid coil.

height (H), mounted in a stainless steel (SUS316L) ring 5 mm in width, was attached to the cold stage of a Gifford-McMahon (GM) cycle helium refrigerator. A copper solenoid magnetizing coil (inner diameter (I.D.) = 100 mm, O.D. = 120 mm, H = 50 mm), which was cooled using liquid nitrogen, was placed outside the vacuum chamber, as shown in Fig. 1. The detailed experimental setup is described elsewhere [9]. After the bulk was cooled to $T_s = 65$ K, a single magnetic pulse, $B_{ex}$, ranging from 3 to 6 T and with a rise time of 13 ms, was applied to the bulk. During PFM, the time dependence of the local field $B_z(t)$ and the final trapped field, $B_t$, were measured using a Hall sensor located at the center of the top surface of the bulk. The time dependence of the temperature, $T(t)$, was measured on the side surface of the SUS316L ring using a CERNOX thermometer.

### B. Numerical Simulation Framework

Based on our experimental setup shown in Fig. 1, a two-dimensional (2-D) numerical model was constructed and numerical simulations were performed using the finite element method (FEM). The physical phenomena during PFM are described by the fundamental electromagnetic and thermal equation in the 2-D axisymmetric coordinate system [10], [11]. Commercial software package, Photo-Eddy, combined with Photo-Thermo (Photon Ltd, Japan) was adopted for the analysis. The simulation procedure and the parameters used are described elsewhere in detail [12].

Fig. 2 shows the $J_c(B, T)$ profiles used in the simulation. The Jirsa model with the peak effect is represented by the following equation [6]:

$$J_c(B, T) = J_{c1}(T)\exp\left(-\frac{B}{B_1(T)}\right) + J_{c2}(T)\frac{B}{B_{\max}(T)} \times \exp\left[\frac{1}{\alpha(T)}\left(1-\left(\frac{B}{B_{\max}(T)}\right)^{\alpha(T)}\right)\right]. \quad (1)$$

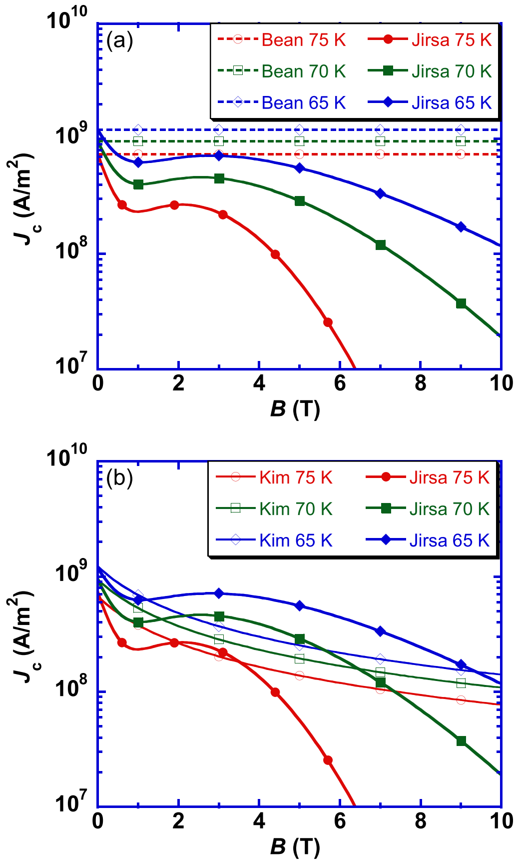


Fig. 2. Magnetic field and temperature dependences of the critical current density, $J_c(B, T)$, between 65 and 80 K used in the simulation for (a) the Jirsa and the Bean models and (b) the Jirsa and the Kim models.

TABLE I
NUMERICAL PARAMETERS FOR THE $J_c$ $(B, T)$ CHARACTERISTICS USING JIRSA MODEL AT 65, 70, 75, AND 80 K IN (1)

| $T$ (K) | $J_{c1}$ (Am$^{-2}$) | $B_1$ (T) | $J_{c2}$ (Am$^{-2}$) | $B_{max}$ (T) | $\alpha$ |
|---|---|---|---|---|---|
| 65 | 1.2 x $10^9$ | 0.57 | 7.6 x $10^8$ | 3.0 | 1.29 |
| 70 | 9.3 x $10^8$ | 0.52 | 4.8 x $10^8$ | 2.5 | 1.62 |
| 75 | 7.5 x $10^8$ | 0.47 | 2.4 x $10^8$ | 1.9 | 2.10 |
| 80 | 6.0 x $10^8$ | 0.42 | 2.6 x $10^7$ | 1.4 | 2.76 |

The experimental $J_c(B, T)$ data [13] were fit up to 10 $T$ between 65 K and 80 K using (1) and the determined parameters ($J_{c1}$, $B_1$, $J_{c2}$, $B_{max}$, and $\alpha$) at each temperature are shown in Table I. The $J_c(B, T)$ profiles at intermediate magnetic field and temperature are interpolated using each parameter.

In the Bean model, the temperature dependence of $J_{c3}(T)$ is assumed to be the following equation, which is the same as $J_{c1}(T)$ in the Jirsa model

$$J_{c3}(T) = J_{c1}(T) = aT^4 + bT^3 + cT^2 + dT + e \quad (2)$$

where $a$, $b$, $c$, $d$, and $e$ are constant values shown in Table II.

In the Kim model, temperature and magnetic field dependence of $J_c(B, T)$ is expressed in the following equation:

$$J_c(B, T) = J_{c4}\left\{1-\left(\frac{T}{T_c}\right)^2\right\}^{\frac{3}{2}} \frac{B_0}{|B| + B_0} \quad (3)$$

TABLE II
NUMERICAL PARAMETERS FOR THE $J_c$ ($T$) CHARACTERISTICS USING BEAN MODEL IN (2)

| *a* | *b* | *c* | *d* | *e* |
|---|---|---|---|---|
| 1.4 x 10² | 5.6 x 10⁴ | 8.3 x 10⁶ | 5.7 x 10⁸ | 1.7 x 10¹⁰ |

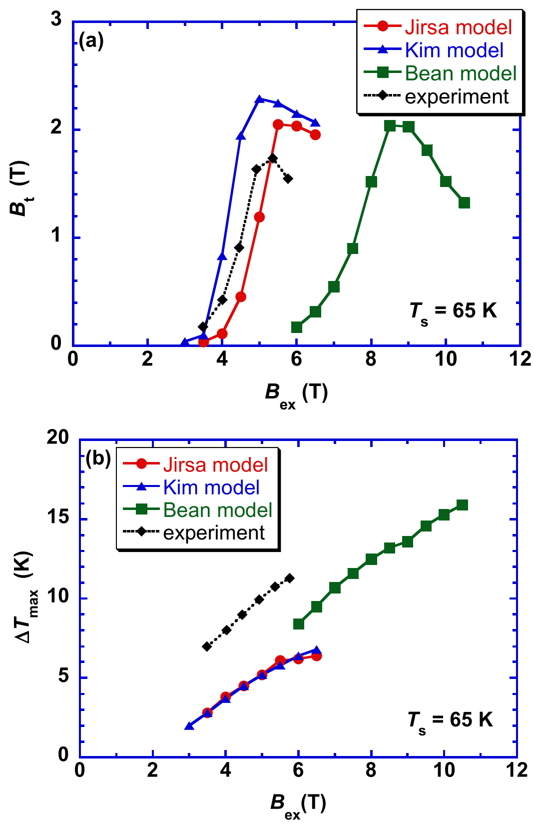


Fig. 3. Applied field dependence of (a) trapped field, $B_t$, at the center of the bulk surface and (b) maximum temperature rise, $\Delta T_{max}$, from 65 K in the numerical simulations using the three kinds of $J_c(B, T)$ characteristics. The experimental results are also shown.

where $B_0 = 1.3$ T is constant and $J_{c4} = 3.45 \times 10^9$ A/m$^2$ is the extrapolated $J_c$ value at $T = 0$ K and $B = 0$ T, which corresponds to $J_c$ (0 T, 65 K) $= 1.2 \times 10^9$ A/m$^2$ and is the same value as that in the Jirsa model. The magnitude of $J_c(B, T)$ values shown in (1)–(3) was adjusted to one third of its small specimen value to adequately reproduce the experimental results [1].

The anisotropic thermal conductivities $\kappa_{ab} = 20\,\mathrm{Wm^{-1}K^{-1}}$ in the *ab*-plane and $\kappa_c = 4\,\mathrm{Wm^{-1}K^{-1}}$ along the *c*-axis of the REBaCuO bulk were assumed to be independent of temperature for simplicity [1]. The temperature dependent thermal conductivity, $\kappa_{SUS}$, and specific heat, $C_{SUS}$, of the SUS316L ring were used [1]. The bulk was cooled to $T_s = 65$ K and the pulsed field, $B_{ex}(t)$ with a rise time of 10 ms was applied. Using the framework, we investigated the trapped field characteristics numerically for these three $J_c$ assumptions.

## III. Results and Discussion

Fig. 3(a) shows the numerical and experimental results of the trapped field, $B_t$, at 65 K at the center of the bulk surface,

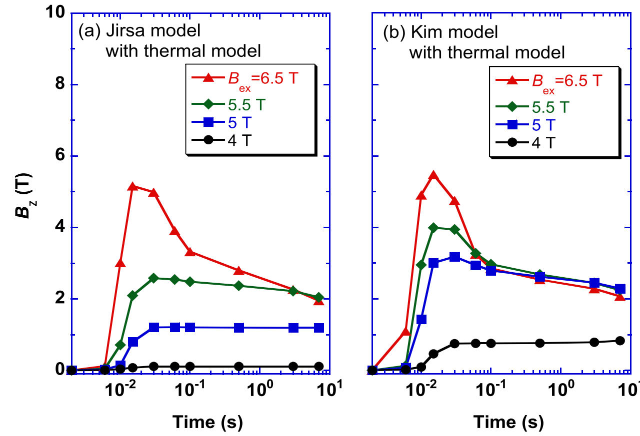


Fig. 4. Time evolution of the local field, $B_z$, for (a) Jirsa model and (b) Kim model at the center of the bulk surface for various applied pulsed fields, $B_{ex}$, in which the temperature changes due to the coupling of the thermal model.

as a function of the applied pulsed field, $B_{ex}$. The experimental results of the $B_t$ versus $B_{ex}$ profile were qualitatively reproduced by the numerical simulation using the Jirsa model, better than when using Bean and Kim models, which suggests that the Jirsa model should be used in the simulation. When the parameters in the Jirsa model are optimized more accurately, the discrepancy may be minimized. Fig. 3(b) shows the maximum temperature rise, $\Delta T_{max}$ from 65 K during PFM, as a function of $B_{ex}$, which was estimated at the same position as that in the experiment shown in Fig. 1. The temperature rise in the simulation increased with the increase in the applied pulsed field, $B_{ex}$. The $\Delta T_{max}$ value of the experiment was larger than that of the simulation. When using the Bean model, the trapped field by FCM is likely to increase, because $J_c$ is not reduced by the presence of the magnetic field. On the other hand, during the PFM process of a Bean model, a larger applied field is necessary for the magnetic flux intrusion into the bulk because of the independence of $B$ in $J_c$. As a result, a larger temperature rise happens after the flux intrusion and then the trapped field is reduced, which is in clear contrast to the FCM process.

It is interesting to consider what kind of $J_c(B, T)$ profile is desired to enhance the trapped field by PFM. For the results of the Kim model, as shown in Fig. 3, the activation field, $B_{ex}{}^*$, which was defined as the magnetic field required to fully magnetize the bulk [9], becomes lower, compared to the Jirsa model. The trapped field of the Kim model is slightly larger because of the moderate $J_c$ degradation with increasing temperature and/or magnetic field. In practical applications, lowering the $B_{ex}{}^*$ value is preferable because the size of the capacitor bank, and ultimately the magnetization fixture, can be reduced. To enhance the trapped field by PFM, a weak temperature dependence of $J_c(T)$ is preferable, rather than the existence of the peak effect in $J_c(B)$.

Fig. 4(a) and (b) shows the time evolution of the local field, $B_z(t)$, at the center of the bulk surface for the Jirsa model and the Kim model, respectively, for various applied fields, $B_{ex}$, in which the temperature variation was permitted (with thermal model). For the Kim model, the magnetic flux is easy to penetrate the bulk center even for lower $B_{ex}$, compared to the Jirsa

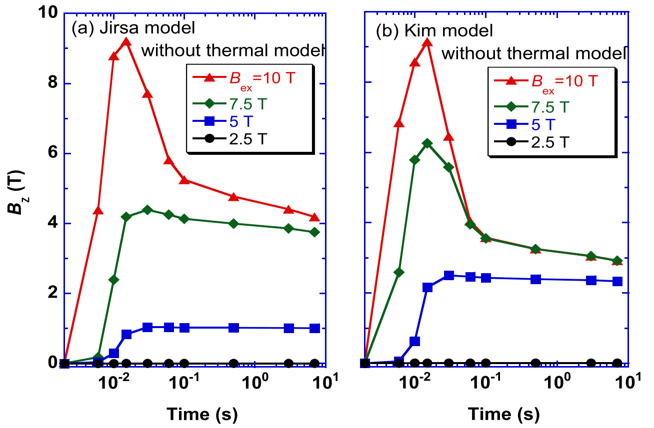


Fig. 5. Time evolution of the local field, $B_z$, for (a) Jirsa model and (b) Kim model at the center of the bulk surface for various applied pulsed fields, $B_{ex}$, in which the temperature is fixed at 65 K assuming isothermal conditions (no thermal model is included).

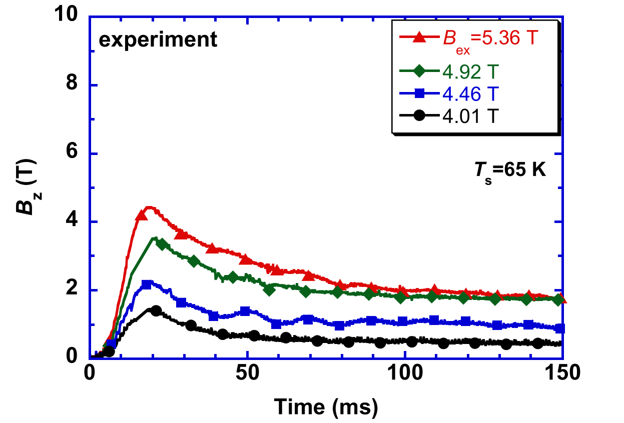


Fig. 7. Experimental results of the time evolution of the local field, $B_z(t)$, at the center of the bulk surface for various applied pulsed fields, $B_{ex}$.

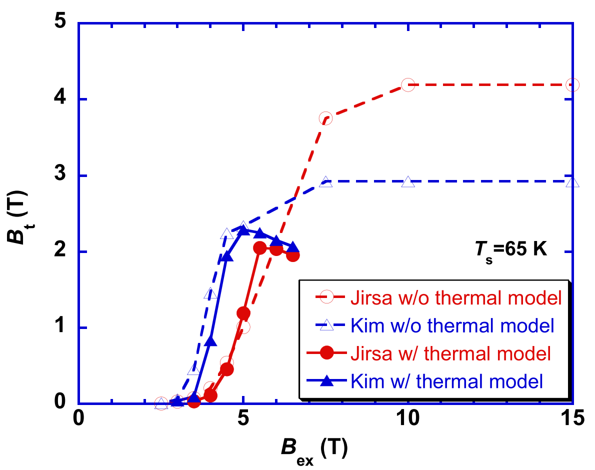


Fig. 6. Trapped field, $B_t$, for the Jirsa and Kim models combined with (w/) and without (w/o) thermal model, as a function of applied pulsed field, $B_{ex}$.

model because of the absence of the peak effect which enhances the pinning strength at intermediate and higher applied field. For higher $B_{ex}$, the time dependence of $B_z(t)$ and the final trapped field, $B_t$, are nearly the same for both models, which may result from the complex relationship between $J_c(B, T)$ and heat generation during PFM.

Fig. 5(a) and (b) shows the time evolution of the local field, $B_z(t)$, at the center of the bulk surface for the Jirsa model and the Kim model, respectively, for various applied fields, $B_{ex}$, in case that the temperature is fixed at 65 K, i.e., isothermal conditions are assumed. The magnetic flux is difficult to penetrate into the bulk center for the lower applied pulsed field because of the absence of temperature rise. As a result, for higher $B_{ex}$ than 7.5 T, the final trapped field for the Jirsa model is higher than that for the Kim model due to the peak effect.

Fig. 6 shows the numerical results for the trapped field, $B_t$, at 65 K, as a function of applied pulsed field, $B_{ex}$, for the Jirsa model and Kim model, in which the results with (w/) and without (w/o) thermal model are shown. When the temperature is fixed at 65 K (w/o) for each model, the activation field, $B_{ex}{}^*$, shifts to high magnetic field and the $B_t$ value increases with increasing the applied pulsed field, $B_{ex}$. The $B_t$ value for the Jirsa model is larger than that for the Kim model due to the peak effect in $J_c(B)$. The $B_t$ value without thermal model is larger than that with thermal model. These results suggest that the presence of the peak in $J_c$ $(B)$ enhances the final trapped field, if the temperature rise is reduced.

Fig. 7 shows the experimental results of the time evolution of the local field, $B_z(t)$, at the center of the bulk surface for various applied pulsed fields, $B_{ex}$. Because of the large temperature rise during the actual PFM, the local field, $B_z(t)$, changes according to the thermal model, as shown in Fig. 4. The $B_t$ value increases with increasing $B_{ex}$. The flux flow at $t > 20$ ms increases with increasing $B_{ex}$ due to the temperature rise. Compared to Fig. 4, the experimental results showed similar trends to the numerical results for higher magnetic fields ($B_{ex} \geqq 5$ T), while the experimental results for lower magnetic fields ($B_{ex} < 5$ T) differed from the numerical results. However, these results suggest that the relationship between the $B_t$ and $B_{ex}$ can be reproduced by numerical simulation.

## IV. Conclusion

The trapped field properties during PFM of a REBaCuO disk bulk were investigated numerically using three different $J_c(B, T)$ characteristics (Jirsa, Kim, and Bean models) and compared with the experimental results. The bulk with the field-independent $J_c$ characteristics like the Bean model, does not achieve higher trapped field by PFM because of a larger temperature rise. In the Jirsa model, the peak effect in $J_c(B)$ is effective to enhance the trapped field, but a steep reduction in $J_c$ with temperature rise can result in a decrease in the trapped field. In the Kim model, the activation field, $B^*_{ex}$, is lower than that for the Jirsa model due to the absence of peak effect and the trapped field is slightly larger than or similar to that for the Jirsa model because of the weak temperature dependence of $J_c$. Therefore, to enhance the trapped field during PFM, $J_c(B, T)$ characteristics with the peak effect and a weak temperature dependence are required. If a REBaCuO bulk with moderate magnetic field and temperature dependences in $J_c(B, T)$ can be fabricated, the trapped field should be enhanced by PFM based on these analyses.

## REFERENCES


[1] M. D. Ainslie *et al.*, "Enhanced trapped field performance of bulk high-temperature superconductors using split coil, pulsed field magnetization with an iron yoke," *Supercond. Sci. Technol.*, vol. 29, no. 7, Jul. 2016, Art. no. 074003.

[2] H. Fujishiro, T. Tateiwa, A. Fujiwara, T. Oka, and H. Hayashi, "Higher trapped field 5 T on HTSC bulk by modified pulse field magnetizing," *Physica C*, vol. 445–448, pp. 334–338, 2006.

[3] M. D. Ainslie *et al.*, "Toward optimization of multi-pulse, pulsed field magnetization of bulk high-temperature superconductors," *IEEE Trans. Appl. Supercond.*, vol. 28, no. 4, Jun. 2018, Art. no. 6800207.

[4] M. D. Ainslie and H. Fujishiro, "Modelling of bulk superconductor magnetization," *Supercond. Sci. Technol.*, vol. 28, no. 5, Mar. 2015, Art. no. 053002.

[5] S. Zou, V. M. R. Zermeno, and F. Grilli, "Influence of parameters on the simulation of HTS bulks magnetized by pulsed field magnetization," *IEEE Trans. Appl. Supercond.*, vol. 26, no. 4, Jun. 2016, Art. no. 4702405.

[6] M. Jirsa, L. Pust, D. Dlouhy, and M. R. Koblischka, "Fishtail shape in the magnetic hysteresis loop for superconductors: Interplay between different pinning mechanisms," *Phys. Rev. B*, vol. 55, 1997, Art. no. 3276.

[7] C. P. Bean, "Magnetization of hard superconductors," *Phys. Rev. Lett.*, vol. 8, 1962, Art. no. 250.

[8] Y. B. Kim, C. F. Hempstead, and A. R. Stmad, "Flux-flow resistance in type-II superconductors," *Phys. Rev.*, vol. 139, 1965, Art. no. A1163.

[9] M. D. Ainslie *et al.*, "Modeling and comparison of trapped fields in (RE)BCO bulk superconductors for activation using pulsed field magnetization," *Supercond. Sci. Technol.*, vol. 27, no. 6, Jun. 2014, Art. no. 065008.

[10] H. Ohsaki, T. Shimosaki, and N. Nozawa, "Pulsed field magnetization of a ring-shaped bulk superconductor," *Supercond. Sci. Technol.*, vol. 15, pp. 754–758, 2002.

[11] Y. Komi, M. Sekino, and H. Ohsaki, "Three-dimensional numerical analysis of magnetic and thermal fields during pulsed field magnetization of bulk superconductors with inhomogeneous superconducting properties," *Physica C*, vol. 469, pp. 1262–1265, 2009.

[12] H. Fujishiro and T. Naito, "Simulation of temperature and magnetic field distribution in superconducting bulk during pulsed field magnetization," *Supercond. Sci. Technol.*, vol. 23, no. 10, Sep. 2010, Art. no. 105021.

[13] T. Kii *et al.*, "Low-temperature operation of a bulk HTSC staggered array undulator," *IEEE Trans. Appl. Supercond.*, vol. 22, no. 3, Jun. 2012, Art. no. 4100904


Authors' biographies not available at the time of publication.